 Cytometry 44:236–246 (2001)

Monitoring Phytoplankton, Bacterioplankton, and Virioplankton in a Coastal Inlet (Bedford Basin) by Flow Cytometry

W.K.W. Li* **and P.M. Dickie**

Biological Oceanography Section, Bedford Institute of Oceanography, Dartmouth, Nova Scotia, Canada

Received 4 October 2000; Revision Received 2 May 2001; Accepted 2 May 2001

Background: To establish the prevailing state of the ecosystem for the assessment of long-term change, the abundance of microbial plankton in Bedford Basin (Nova Scotia, Canada) is monitored weekly by flow cytometry.
Methods: Phytoplankton are detected by their chlorophyll autofluorescence. Those that contain phycoerythrin are designated as *Synechococcus* cyanobacteria or cryptophyte algae according to the intensity of light scatter. Bacteria and viruses are stained with DNA-binding fluorochromes and detected by green fluorescence. Distinction is made between bacterial and viral subpopulations exhibiting high and low fluorescence.
Results: Time series data are presented for weekly observations from 1991 to 2000. Weekly averages are computed for the complete annual cycle of temperature, salinity, river discharge, nitrate, phosphate, silicate, chlorophyll, total phytoplankton including *Synechococcus* and cryptophytes, total bacteria including high and low-fluorescence subpopulations, and total viruses including high and low-fluorescence subpopulations.
Conclusions: The microbial biomass in the surface water of Bedford Basin is dominated by phytoplankton. The spring bloom of phytoplankton represents a maximum in algal biovolume, but not in cell number. Phytoplankton, bacteria, and viruses all attain their annual numerical maxima between the summer solstice and the autumn equinox. A vigorous microbial loop and viral shunt is envisioned to occur in the summer. Cytometry 44:236–246, 2001. © 2001 Wiley-Liss, Inc.

Key terms: Bedford Basin; phytoplankton; bacteria; virus; *Synechococcus*; cryptophytes; chlorophyll; marine ecosystem monitoring; coastal inlet; flow cytometry

In earth sciences, the measurement of state variables at regular and frequent intervals sustained over a long time at a fixed location provides valuable information on change at various temporal scales. Many important issues of scientific and societal concern can be addressed only with multiyear time series data (1). These issues have provided the impetus to initiate, sustain, or expand observations that monitor the state of marine ecosystems. For inshore coastal waters, especially those adjacent to centers of human population, there is an urgency to detect and predict the effects of natural and anthropogenic changes on marine biota (2).

In eastern Canada, a program to monitor the continental shelves of the northwest Atlantic Ocean (3) includes time series observations at several inshore locations, of which the most well-studied is Bedford Basin. This basin is a small marine embayment that constitutes the inner component of the Halifax inlet system and is surrounded by the largest urban population in eastern Canada. Coastal monitoring programs are conducted at many oceanographic institutions (1,4,5) but only a few include observations of microbial components other than phytoplankton. There is no doubt that picoplankton (heterotrophic bacteria and small photoautotrophic algae) and femtoplankton (viruses) are important components of many plankton communities, including those in coastal waters (6–9). However, to our knowledge, there are few sustained records of the contemporaneous abundance of phytoplankton, bacterioplankton, and virioplankton.

In 1991, we began to monitor weekly the abundance of plankton in Bedford Basin. We present the time series observations and the computed weekly climatologies for the abundances of microbial plankton enumerated by flow cytometry (FCM). These results establish firmly the mean state of the basin in the 1990s against which future changes can be compared. Additionally, the results allow a general examination of the microbial components in relationship to each other and to their physicochemical environment at a weekly time scale for the complete annual cycle.

*Correspondence to: William Li, Biological Oceanography Section, Bedford Institute of Oceanography, P.O. Box 1006, Dartmouth, Nova Scotia, Canada B2Y 4A2.
E-mail: LiB@mar.dfo-mpo.gc.ca

MATERIALS AND METHODS

Study Site

Bedford Basin in Nova Scotia has a surface area of 17 km^2 and a volume of 5.6×10^8 m^3. It is connected to the open Atlantic Ocean by a channel that is about 10 km long and only 400 m wide at its narrowest part. The deepest point in the basin is 70 m, but the channel is shallower than the basin and constitutes a sill that is 20 m deep. Freshwater enters as discharge from the Sackville River and as runoff from the surrounding areas. Over the past three and a half decades, the location of our laboratory on the shore of the basin has facilitated many studies. A bibliography of the basin is available (10). However, it fails to include studies of general scientific principles that could have been actualized in any easily accessible body of water (11–17).

Water and Data Collection

The Compass Buoy station (44° 41′30″N, 63° 38′30″W) has been occupied by a small boat almost every Wednesday morning since October 16, 1991. Seawater samples are collected by Niskin bottle. Beginning March 10, 1993, depth profiles of temperature, salinity, photosynthetically active radiation (PAR), and in vivo chlorophyll fluorescence have been logged by a Seabird SBE 25-03 CTD system equipped with a pressure sensor SBE-29-300. Temperature is recorded by sensor SBE-3-01/F; conductivity by sensor SBE-4-01/0; PAR by LiCor underwater LI 193SA spherical quantum sensor; in vivo fluorescence of chlorophyll *a* by Wetlabs Wetstar miniature fluorometer set to a range of 0.03–30 mg m^{-3} range; and dissolved oxygen by SBE-23Y polarographic type sensor with replaceable membranes (YSI 5739). The CTD system is lowered at a rate of approximately 1 m s^{-1}. Measurements of discharge from the Sackville River (44° 43′53″N, 63° 39′45″W) were extracted from records of the Atmospheric Environment Branch of Environment Canada.

Sample Analyses

Samples of inorganic nutrients are stored frozen in acid-washed plastic vials. Nitrate, phosphate, and silicate are measured by an autoanalyzer (Technicon II or Alpkem RFA300) and calibrated against KNO_3, KH_2PO_4, and Na_2SiF_6 (18). Chlorophyll *a* is measured in vitro by the fluorescence (Turner Design Model 10 fluorometer) of 90% acetone extracts of plankton filtered onto Whatman GF/F filters and calibrated against the pigment from spinach.

Samples (2 mL) for FCM cell analyses are fixed in 1% paraformaldehyde for 10 min at room temperature and stored at -80°C in cryogenic vials (19). Analyses are performed using a FACSort (Becton Dickinson, San Jose, CA) equipped with a 488-nm argon-ion laser. Sample flow rate (mL s^{-1}) is determined by linear calibration of volume aspirated against analysis duration (20). Standard protocols are used to enumerate phytoplankton (including the cyanobacterium *Synechococcus* and cryptophyte algae), heterotrophic bacteria, and viruses (21,22).

Phytoplankton

Phytoplankton are detected by their native chlorophyll autofluorescence. The sample is vigorously swirled using a vortex mixer to disaggregate cells linked in chains. An aliquot of less than 0.5 mL is analyzed, thus only cells present in substantial numbers are counted (10 or more per milliliter). Because the abundance of cells is inversely related to cell size (23), this generally restricts our detection of phytoplankton to cells in the picoplankton (<2 μm) and nanoplankton (>2 μm, <20 μm) size ranges. The inability to account adequately for the microphytoplankton (>20 μm) will be discussed later.

Some of the detectable phytoplankters show orange autofluorescence, which indicates the presence of phycoerythrin. Following a standard protocol (21,22), we discriminate the orange fluorescence cells based on size: those in the picoplankton are designated *Synechococcus* cyanobacteria and those in the nanoplankton are designated cryptophyte algae. All other phytoplankters remain unclassified by taxonomic affiliation. The picoplanktonic cyanobacterium *Prochlorococcus* is primarily an oceanic genus, although it has been documented in some coastal waters (24). We have not detected *Prochlorococcus* in Bedford Basin. Phycocyanin-rich cyanobacteria cannot be discriminated from other cells without red excitation light. If present in Bedford Basin, they would have been detectable under the optical configuration used (25) and included in the count of total red-fluorescing phytoplankters.

Measurements of cytometric forward light scatter allow us to estimate the biovolume and mean equivalent spherical diameter (ESD, μm) of the phytoplankton assemblage. We calibrated light scatter against particle volume using synthetic beads (26). However, differences in shape and refractive index between cells and beads may reduce the accuracy of the calibration. Accepting this uncertainty, we computed total biovolume (V) from measurements of abundance (n) and estimates of cell volume (v) over the full cytometric range of 256 data channels (i), thus:

$$V = \sum n_i v_i \tag{1}$$

The average ESD is then calculated directly from the average total biovolume ($\bar{V}$):

$$\bar{V} = \frac{V}{\sum n_i} \tag{2}$$

$$\mathrm{ESD} = \sqrt[3]{\frac{6\bar{V}}{\pi}} \tag{3}$$

Finally, we estimated the chlorophyll biomass represented by the phytoplankton (Chl'). We converted cell volume to cell carbon (27) and then converted cell carbon to chlorophyll using a factor of 40 (28):

$$\mathrm{Chl}' = \sum n_i \frac{[0.433(v_i)^{0.863}]}{40} \quad (4)$$

Bacterioplankton

In 1992, we counted bacteria by epifluorescence microscopy of cells stained with DAPI (Sigma, St. Louis, MO; 15). Subsequently, we counted bacteria by FCM using fluorochromes from Molecular Probes (Eugene, OR): TOTO-1 (15) from 1993 to 1995, SYTO-13 (29) from 1996 to 1998, and SYBR Green I (30) from 1999 to 2000. This succession of stains represents an evolution toward increased signal sensitivity and ease of sample preparation (22). We confirmed that there were no significant differences in bacterial counts according to the stain used. In all samples, at least two subpopulations of bacteria can be distinguished by the intensity of green fluorescence (15). Following Gasol et al. (31,32), we refer to these as high DNA (HDNA) and low DNA (LDNA) bacteria and presume that the former are metabolically more active. The abundances of these subpopulations are obtained by Gaussian deconvolution of the green fluorescence frequency histogram using Peakfit™ (SPSS, Chicago, IL).

Virioplankton

Samples for FCM enumeration of viruses are diluted in Tris-EDTA buffer and stained with SYBR Green I (33,34). We applied this newly developed method to retrospective analysis of samples in cryogenic storage since 1996. In all samples, at least two subpopulations of viruses can be distinguished by the intensity of the green fluorescence (33). Following Marie et al. (22,33), we refer to the high-fluorescence viruses as type I and the low-fluorescence viruses as type II. It is speculated V-I may be phytoplankton viruses, whereas V-II may be bacterial viruses (33). The abundance of these subpopulations is obtained by Gaussian deconvolution of the green fluorescence frequency histogram using Peakfit.

RESULTS

Physicochemical Environment

The weekly records of water temperature, salinity, and river discharge (Fig. 1) and of inorganic nutrients (Fig. 2) indicate interannual differences in magnitude, but a consistent pattern of seasonal variation from year to year. The weekly averages (over all years) of these variables depict a stereotypic temperate coastal embayment (Fig. 3). At a depth of 5 m, water temperature is lowest in mid February and highest in early September. Salinity is highest in summer, coinciding with the period of lowest river runoff and highest temperature. Inorganic nutrients decrease in the spring and increase in the fall. Nitrate (but not phosphate or silicate) approaches or reaches the limits of analytical detection in the summer.

Phytoplankton

FCM counts of phytoplankton (Fig. 4A), including *Synechococcus* (Fig. 4B) and cryptophytes (Fig. 4C), indicate late summer peaks in abundance. In successive years since

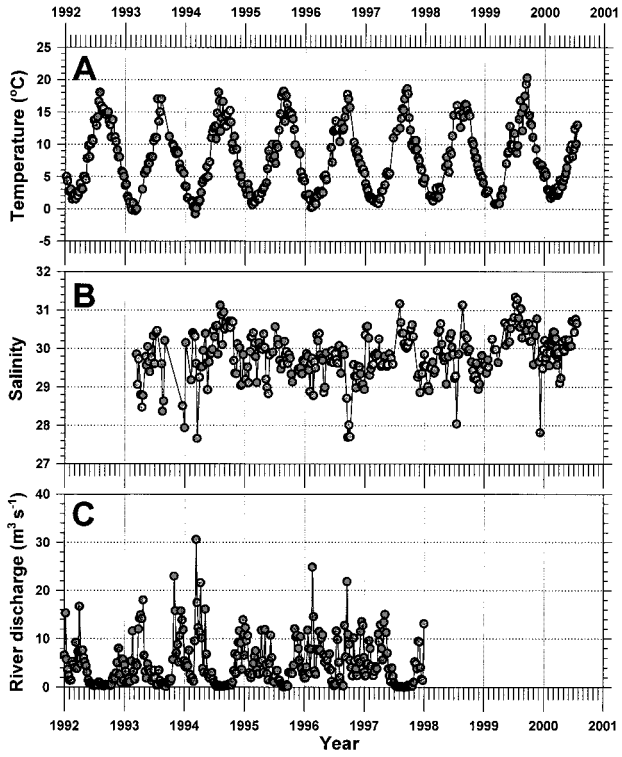

FIG. 1. Time series of **A:** temperature and **B:** salinity at 5 m in Bedford Basin. **C:** Time series of Sackville River discharge.

1993, these annual peaks have increased in magnitude. The weekly averages indicate that the timing of the annual minimum and maximum of phytoplankton abundance (Fig. 5A) is coincident with temperature (Fig. 3A). The seasonal variation in *Synechococcus* is notably different in its sustained decline from a maximum in late summer to a minimum in late spring of the following year (Fig. 5B). For cryptophytes, the major peak in late summer (coincident with that of other phytoplankters at about week 37) is preceded by a slightly less intense peak in late spring at week 21 (Fig. 5C).

On average for the phytoplankton, there is a long period of increase from late winter to the autumn equinox (Fig. 5A,D) that progresses at a net rate of about one doubling every 40 days. For *Synechococcus*, the period of increase is substantially shorter, being confined to the summer (Fig. 5B), and progresses at a net rate of about one doubling every 9 days. For cryptophytes, there is only a 10-fold increase from minimum to maximum (Fig. 5C) and this progresses at a net rate of about one doubling every 80 days.

The distinction between phytoplankton abundance (cells mL^{-1}) and biomass (estimated from biovolume or measured as bulk chlorophyll) is extremely important. Often, a few large cells can exceed the mass of many small cells. Figure 6 is a sequence of flow cytograms that show the development of phytoplankton in 1996. In March, the phase-space of red fluorescence versus forward light scatter shows cell clusters in the upper right corner, which

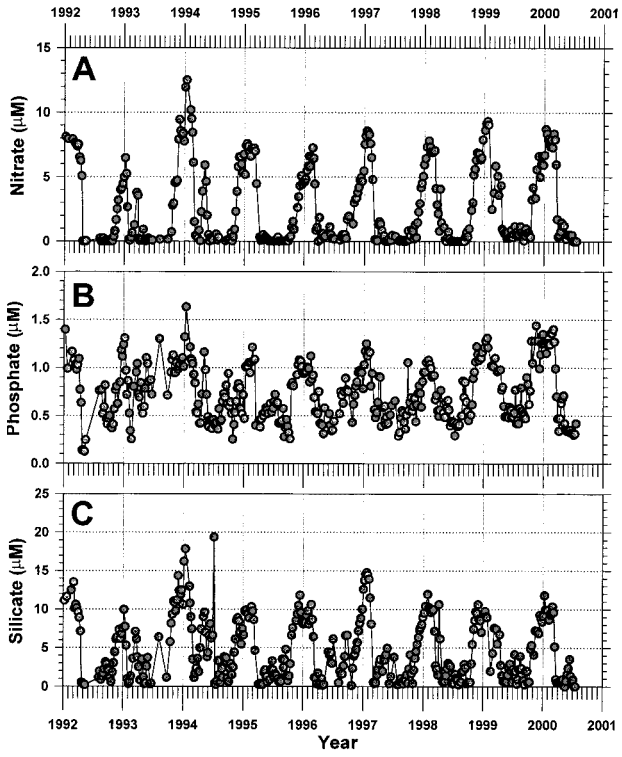

FIG. 2. Time series of **A:** nitrate, **B:** phosphate, and **C:** silicate at 5 m in Bedford Basin.

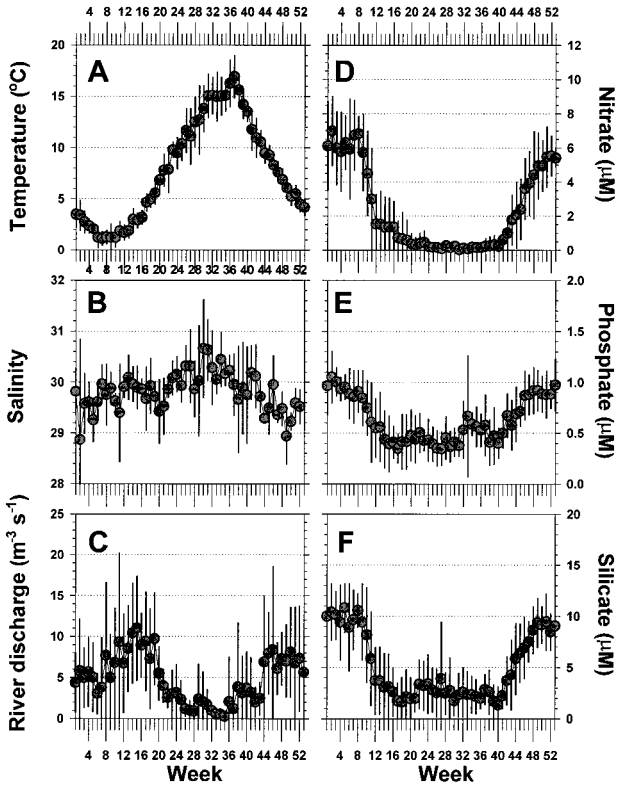

FIG. 3. Weekly average **A:** temperature, **B:** salinity, **C:** river discharge, **D:** nitrate, **E:** phosphate, and **F:** silicate at 5 m in Bedford Basin. Error bars represent SD.

indicates a moderate number of large, chlorophyll-rich cells. By contrast, in August, there are extensive cell clusters in the center and lower left corner of the phase-space, which indicate a much larger number of smaller, chlorophyll-poor cells.

In numerical terms, the late summer peak in phytoplankton is 50% *Synechococcus* (see Fig. 10D). Because of their small size, the average ESD of the entire assemblage is reduced during this time of year (Fig. 5E). By contrast, the late spring peak in cryptophytes comprises only 10% of the phytoplankton (see Fig. 10E). Their ESD (about 10 μm) does not greatly influence the assemblage ESD (Fig. 5E). The prototypic spring bloom of phytoplankton manifests at about week 11. Although the cells are few (Fig. 5D), they are large (Fig. 5E) and constitute a maximum in biovolume (Fig. 5F).

Bacterioplankton

The time series data of bacterioplankton indicate a range in abundance from 3×10^5 to 9×10^6 cells mL^{-1} (Fig. 7A). Both subpopulations of HDNA and LDNA bacterioplankton undergo seasonal variations of about one order of magnitude (Fig. 7B,C), even though the LDNA bacterioplankton is thought to be metabolically less active than HDNA bacterioplankton (15,31,32).

Weekly averages indicate an early summer maximum at week 26 (see Fig. 9A–C). There is no clear seasonal pattern in the percentage of bacteria belonging to each subpopulation. HDNA varies between 58% and 78% of the total bacterioplankton (see Fig. 10A), whereas LDNA forms the complement.

Virioplankton

The time series data of virioplankton (Fig. 8A) resemble closely those of bacterioplankton (Fig. 7A), except that the abundances are much higher. It is notable that the peak abundances of these microbial components are ranked identically in the 4-year period from 1996 to 1999. Thus, the summer peaks of bacterioplankton and virioplankton were highest in 1996, less in 1999, and lowest in 1997 and 1998. Subpopulations V-I and V-II display summer maxima and winter minima (Fig. 8B,C).

Weekly averages of total virioplankton (Fig. 9D) and the subpopulations (Fig. 9E,F) indicate an annual variation of about one order of magnitude. There is no clear seasonal pattern in the percentage of viruses that belong to each subpopulation. V-II varies between 76% and 87% of the total virioplankton (Fig. 10B), whereas V-I forms the complement. The ratio of virioplankton to bacterioplankton varies between 4 in the winter to 17 in the summer, averaging 7 for the year (Fig. 10C).

Chlorophyll

Chlorophyll, as a bulk measure of total phytoplankton biomass irrespective of size, provides the conventional

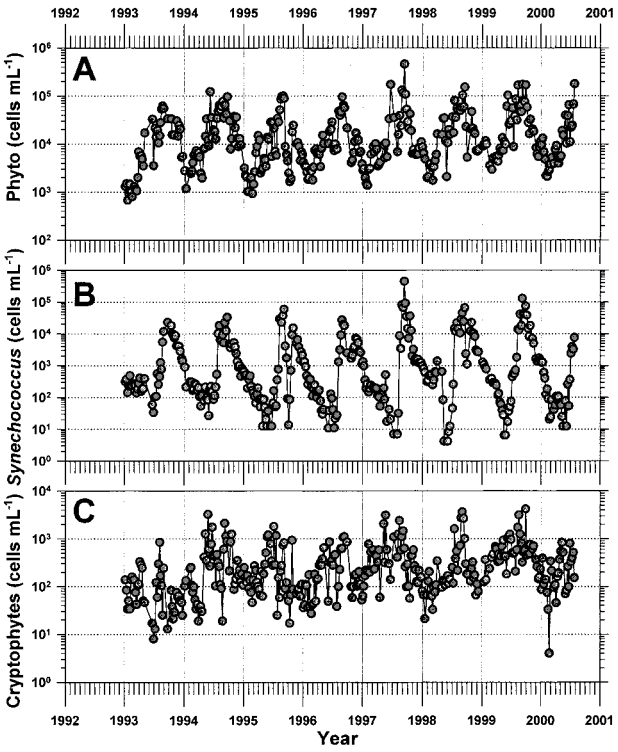

FIG. 4. Time series of **A:** phytoplankton, **B:** *Synechococcus*, and **C:** cryptophyte algae at 5 m in Bedford Basin, measured by FCM.

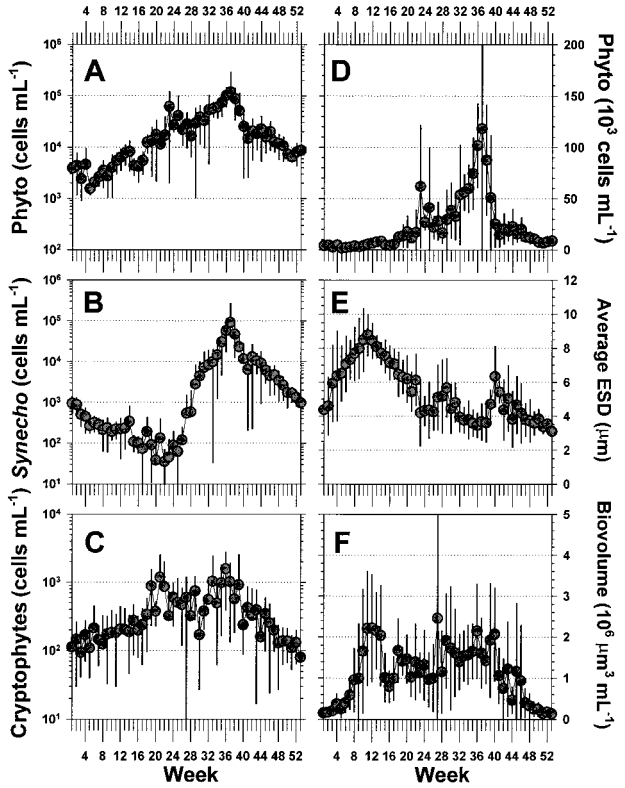

FIG. 5. Logarithmic plots of weekly average abundance of **A:** phytoplankton, **B:** *Synechococcus*, and **C:** cryptophyte algae at 5 m in Bedford Basin. Linear plots of weekly average abundance of **D:** phytoplankton, **E:** their average ESD calculated from Equation 3, and **F:** their biovolume calculated from Equation 1. Error bars represent SD.

depiction of photoautotrophic development in the ocean. The time series data of chlorophyll in Bedford Basin (Fig. 11A) indicate substantial interannual variability in seasonal progression. For example, the 1992 spring bloom was late (week 17) and weak (7 mg m^{-3}), whereas it was early (week 4) and intense (28 mg m^{-3}) in 1993. In the fall, there may be short-lived bloom events that reach unusually high levels (e.g., 109 mg m^{-3} in week 32 in 1993) or there may be long-lived, low-level development of chlorophyll from summer to winter (which occurred in 1996).

FCM makes it possible, in principle, to recover the bulk properties from a knowledge of the constituent properties. In our study, we compute the bulk chlorophyll concentration implied by the measured abundance of phytoplankton in 256 cytometric size classes, their estimated cell volume, an allometric relationship to convert cell volume to cell carbon, and a best-guess factor to convert cell carbon to cell chlorophyll (see Materials and Methods). On a weekly average basis, these calculations of chlorophyll (Fig. 11C) are remarkably similar to measured averages (Fig. 11B). Notable differences are the underestimation of the spring bloom (weeks 10–12), as well as of unusually intense fall events (week 32), and the overestimation of the summer minimum (weeks 27–30).

A comparison is made of the three microbial pools expressed in common units of mgC m^{-3} (Table 1). Throughout the year, the surface layer in Bedford Basin is dominated by phytoplankton biomass.

DISCUSSION

A goal shared by many monitoring programs is the detection of long-term changes in key variables. Measurements must be made over time to establish the prevailing state and the degree of existing variability. Subsequent measurements may be compared against the climatological averages to detect anomalies. In our 8.5-year record for Bedford Basin, we discerned annual increases in temperature and phytoplankton abundance (Figs. 1, 4). However, in this study, we focus our discussion only on the weekly average state of the annual cycle, deferring the analysis of long-term trends to a later contribution. We examine the microbial components in relationship to each other and to their physicochemical environment, not for any particular year, but for the 52-week cycle averaged from the complete time series data.

The annual cycle of phytoplankton biomass in temperate coastal waters has been documented since the earliest days of biological oceanography. It is regulated by seasonal changes in water column mixing and stratification. Traditionally, phytoplankton have been monitored by chemical assay of a bulk algal constituent such as chlorophyll or by microscopic examination, which yields a detailed floristic description. More recently, remote sensing measurements of surface ocean color map phytoplankton

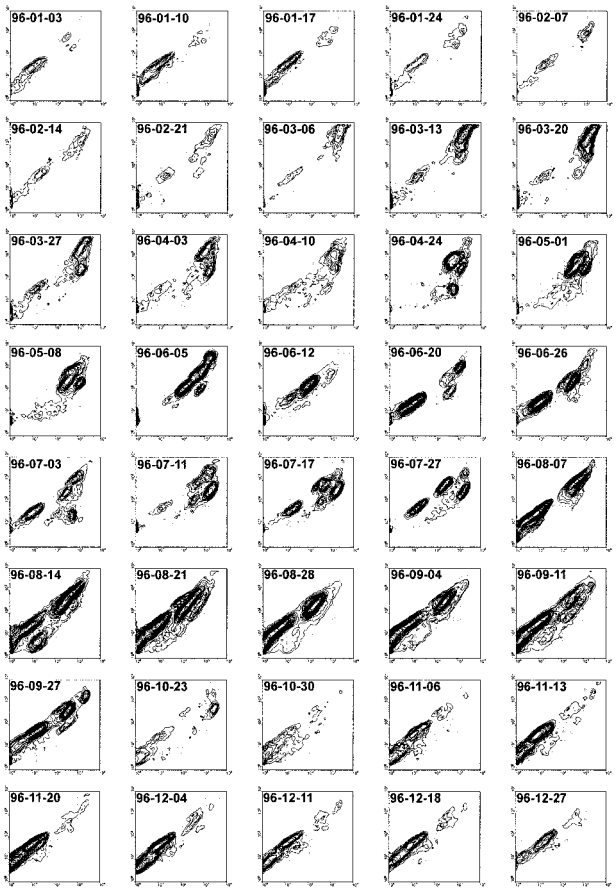

FIG. 6. Flow cytograms of phytoplankton development in 1996. Each panel shows the signature of red fluorescence (ordinate) versus forward light scatter (abscissa), using a four-decade logarithmic scale on each axis. Contours are constructed from the 50% logarithmic algorithm of WinMDI 2.8 (©Joseph Trotter). The date of sampling is indicated in year-month-day format.

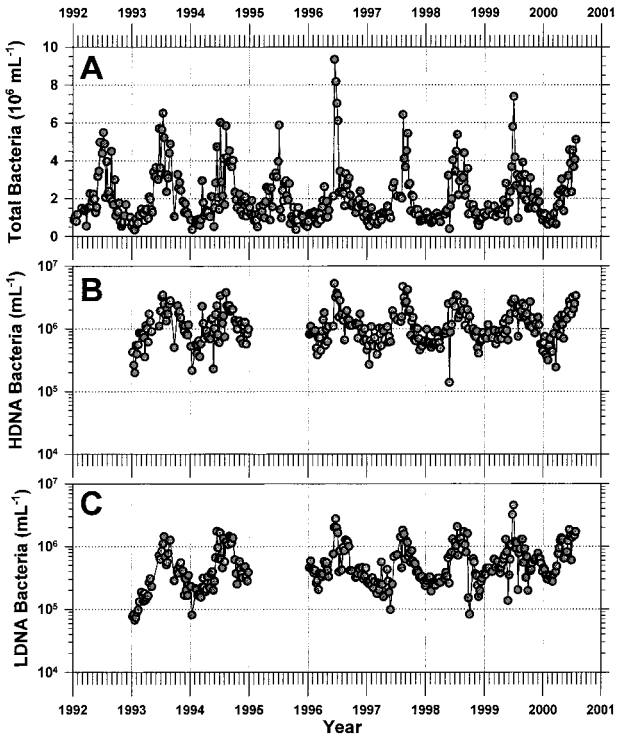

FIG. 7. Time series of of **A:** total bacteria (linear), **B:** HDNA bacteria (logarithmic), and **C:** LDNA bacteria (logarithmic) at 1 m in Bedford Basin. In 1992, total counts were made by epifluorescence microscopy of DAPI-stained cells without discrimination of subpopulations. In 1995, counts were made by FCM analysis of TOTO-stained cells, but the listmode files were inadvertently lost before the analysis of subpopulations.

by proxy (35). Enumeration of microorganisms by FCM cannot match the spatial resolution provided by satellites or the taxonomic resolution provided by microscopy. However, FCM affords many unique advantages and is accepted widely as a versatile tool in modern oceanography (36). It is used increasingly to construct time series of phytoplankton development (37,38). Already, unattended flow cytometers designed for submersible moored operation are pointing to new opportunities for plankton monitoring (39,40).

Our measurements of phytoplankton, bacterioplankton, and virioplankton from separate aliquots of a 2-mL cryopreserved sample delineate the scope of FCM analyses (22). We do not have a routine FCM protocol to account for the protozoans, which are additional crucial members of the microbial plankton. Existing research methods that rely on oligonucleotide probes (41,42) are impractical to implement for monitoring. However, a new protocol for FCM enumeration of heterotrophic nanoflagellates (43) uses a modification of the conventional bacterioplankton method, which may allow us to extend the inventory of microbes.

Bedford Basin is connected to the adjacent continental shelf through a sill and a long channel. The exchange of shelf and inshore water, largely caused by alongshore winds driving Ekman transport, exerts strong control of the nutrient (44) and chlorophyll (45) regimes in the basin. From considerations of physiography and water exchange at the inlet mouth, it has been estimated that for time scales longer than about 3 days, Bedford Basin loses its autonomy as an independent ecological unit because external physical forces dominate the intrinsic biological dynamics (46). At shorter time scales, aperiodic events occur in which local biological signals may override general seasonal patterns. These include exceptional events of red-water discoloration attributed to the dinoflagellates *Gonyaulax digitale* (47) and *Dinophysis norvegica* (48). However, at the time scale of 1 week, the computed climatologies in Bedford Basin may be reasonable exemplars of the adjacent shelf. Average nutrient concentrations in Bedford Basin (Fig. 3) are similar to those in the central Scotian Shelf (49). Further, primary production in Bedford Basin, as on the shelf, is dominated by phytoplankton without significant contribution from seaweed or seagrass as in some neighboring inlets of different morphometry (50). The coupling of Bedford Basin to the

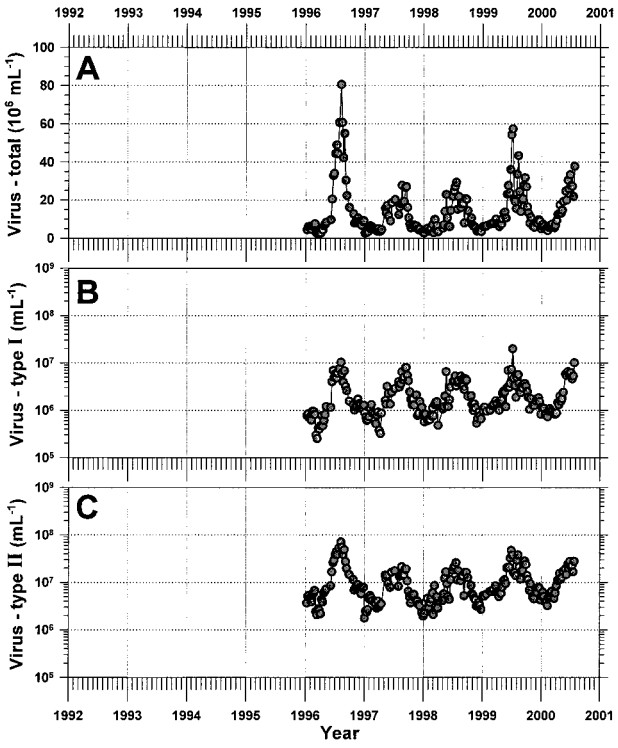

FIG. 8. Time series of of **A:** total virus (linear), **B:** high-fluorescence V-I (logarithmic), and **C:** low- fluorescence V-II (logarithmic) at 1 m in Bedford Basin, measured by FCM.

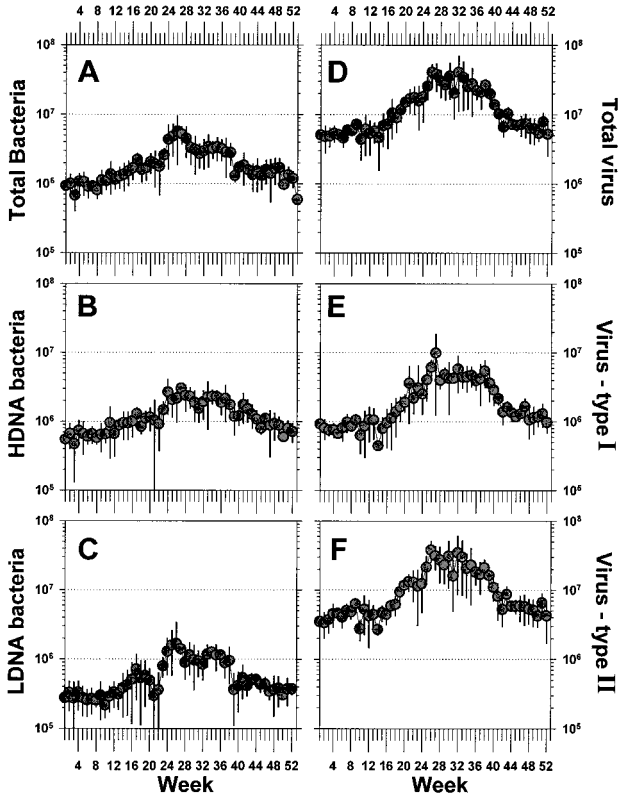

FIG. 9. Weekly average abundance of **A:** total bacteria, **B:** HDNA bacteria, **C:** LDNA bacteria, **D:** total virus, **E:** V-I, and **F:** V-II at 1 m in Bedford Basin. Error bars represent SD.

adjacent continental shelf at longer time scales (46) suggests that there may be close similarities in the annual sequence of recurring biological events, and perhaps some concordance in year-to-year trends.

The annual plankton cycle in Bedford Basin begins after week 7 or 8 when the water temperature is at a minimum (Fig. 3). Solar radiation increases and surface warming begins to stabilize the water column, which has been intensely mixed over the winter. These factors initiate the spring bloom of phytoplankton in temperate waters (6), which may begin earlier in Bedford Basin than offshore (12). Nutrients (Fig. 3) decrease rapidly from their winter maxima to supply the growth of phytoplankton biomass (chlorophyll), which reaches a peak at week 11 or 12 during the spring equinox (Fig. 11B).

The spring bloom is a peak in the biomass, or biovolume, of the phytoplankton (Fig. 5F), and not in their numbers (Fig. 5D). At this time of year, cells are at their largest average size (Fig. 5E) and therefore constitute a large biovolume. Previous studies (51–54) have shown that the bloom includes diatoms, dinoflagellates, silicoflagellates, cryptophytes, and others; centric diatoms such as *Chaetoceros* spp., *Thalassiosira* spp., and *Skeletonema costatum* are dominant. It is likely that these earlier studies failed to give a complete account of the bloom. For example, Taguchi and Platt (51) made microscope counts of Lugols-preserved phytoplankton sampled at biweekly intervals throughout 1974. A plot of these historical data (not shown) reveals an annual development strikingly similar in appearance to the FCM weekly averages (Fig. 5A). However, the earlier estimates of abundance are from 100 to more than 1,000 times less than the FCM values. Phytoplankton biovolumes calculated from light microscopy fail to mimic the annual cycle of bulk chlorophyll measured in 1974, in distinct contrast to the match derived from current FCM measurements (Fig. 11C). Subsequently, Lehman (52) also noted that flagellates, not diatoms, comprise the numerical majority in the Bedford Basin spring bloom. In waters elsewhere, the green of the spring bloom is likewise not attributable wholly to diatoms: evidence from Continuous Plankton Recorders points to phytoflagellates (53); evidence from chromatographic pigment analysis points specifically to cryptophytes (54); and evidence from size fractionation of chlorophyll points to a large contribution from small cells (7).

At the peak of the spring bloom in Bedford Basin during the week of the equinox, the average chlorophyll concentration is 14 mg m^{-3} (Fig. 11B). FCM measurements account for 10 mg m^{-3} (Fig. 11C), in the form of about 5,500 phytoplankters mL^{-1} (Fig. 5D), of which 6% are *Synechococcus* (Fig. 10D) and 4% are cryptophytes (Fig. 10E). In other words, 30% of the biomass is unaccounted and 90% of the cells are unidentified. The unaccounted biomass is

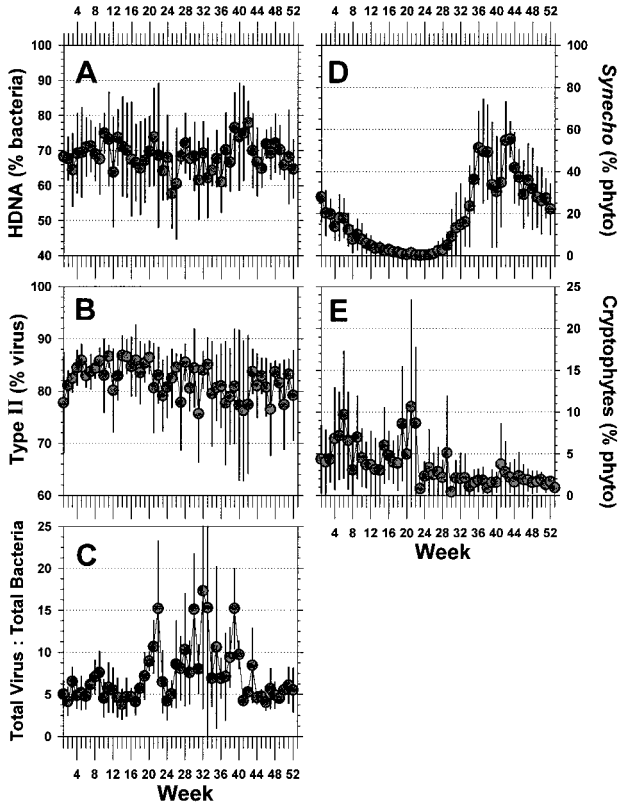

FIG. 10. Weekly average values for ratios. **A:** HDNA as a percentage of total bacteria, **B:** V-II as a percentage of total virus, **C:** ratio of total virus to total bacteria, **D:** *Synechococcus* as a percentage of total phytoplankton, **E:** cryptophyte algae as a percentage of total phytoplankton.

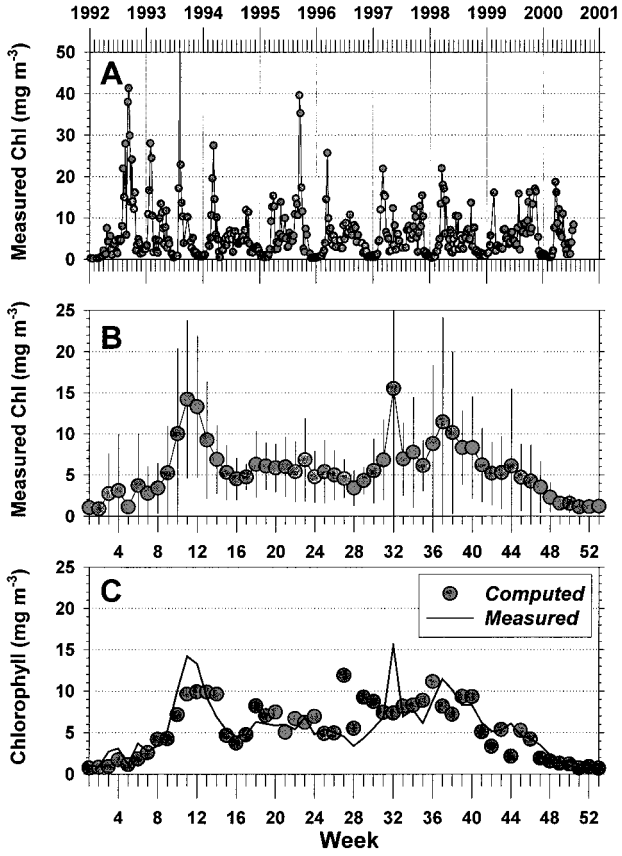

FIG. 11. **A:** Time series of bulk chlorophyll concentration at 5 m in Bedford Basin. The offscale value in 1993 was measured on August 6 at 109 mg m^{-3}. **B:** Weekly average concentration of measured chlorophyll. Error bars represent SD. **C:** Weekly average concentration of chlorophyll calculated using FCM measurements in Equation 4 (circles) compared with bulk values (solid line) measured directly in (B).

undoubtedly in the form of microphytoplankton cells or nanoplankters in chains, both of which are too large to be detected by the FACSort instrument. Unfortunately, many chain diatoms and other species (e.g., toxin producers, nonindigenous invaders) are poorly reconciled in FCM analysis.

Of the nearly 5,000 phytoplankters mL^{-1} that we can count and size but not identify, some are undoubtedly the flora identified by previous workers. Yet, the phytoplankton identified by microscopy in early studies (13,52,55) do not usually total more than about 1,000 cells mL^{-1} in the spring. Up to 80% of the springtime phytoplankters enumerated by FCM may have been missed by conventional methods. Samples fixed in buffered paraformaldehyde and stored at a cryogenic temperature contain many phytoplankters detectable by FCM that are otherwise lost by preservation in Lugol's fixatives. High-performance liquid chromatographic analysis of pigments indicates that the spring bloom complement consists largely of fucoxanthin (EJH Head, personal communication), which is present in diatoms, prymnesiophytes, chrysophytes, and raphidophytes (56). Many of the flagellates in the latter classes are fragile and difficult to preserve, but may dominate the phytoplankton at certain times of the year (56). Very high phytoplankton abundances exceeding 10^4 cells mL^{-1} were recorded in the spring of 1995 when samples preserved by gentle fixation (1:1 glutaraldehyde and paraformaldehyde at 1%) were examined microscopically (57).

The period of spring from the equinox to the summer solstice (week 25 or 26) is a time of intense microbial

Table 1
*Standing Stocks of Microbial Carbon in Surface Waters of Bedford Basin**

Week	Period	Phytoplankton	Bacteria	Virus
12	Spring equinox	532	34	1
25	Summer solstice	216	145	5
38	Autumn equinox	405	84	5
51	Winter solstice	44	40	2
1 → 52	Annual average	223	61	3

*Standing stocks are in units of mgC m^{-3}. Phytoplankton carbon is calculated from chlorophyll using C:Chl ratio of 40 (28). Bacterial carbon is calculated from bacterial abundance using a cellular content of 30 fgC $bacterium^{-1}$ (68). Viral carbon is calculated from viral abundance using a particle content of 0.2 fgC $virus^{-1}$ (69).

growth, even as bulk chlorophyll decreases. The total number of phytoplankton cells increases (Fig. 5A), in small part due to cryptophytes (Fig. 5C), and in spite of a decrease in *Synechococcus* (Fig. 5B). All the bacteria and viruses increase at sustained rates to respective maxima at the summer solstice (Fig. 9). Microzooplankton biovolume also increases (58). There is an increased flux of regenerated nutrients throughout this period, but this is largely balanced by the flux of uptake as spring progresses (59).

The summer, from the solstice to the autumn equinox (week 37 or 38), is perhaps the most interesting part of the year from a microbial point of view. The thermocline is formed fully and surface nitrate approaches undetectable limits (Fig. 3D), but ammonium is available as a result of microbial regeneration. The levels of both bacteria and viruses decrease slightly from their maxima but remain relatively abundant throughout the summer (Fig. 9). This is also the time of year when the ratio of viruses to bacteria is highest (Fig. 10C). The weekly average concentration of chlorophyll increases, building to a peak (the fall bloom) in September (Fig. 11B). Throughout the summer, primary production is at levels almost as high as in the spring (60,61). Short-lived blooms of dinoflagellates are not unusual (47,48), but they do not recur with annual regularity. One such bloom in 1993 led to the highest value of chlorophyll recorded in this basin (Fig. 11A).

Summer culminates in the autumn equinox when water temperature at 5 m is at its highest average value for the year (Fig. 3A). This is the time of maximum total phytoplankton (Fig. 5A), *Synechococcus* (Fig. 5B), and cryptophytes (Fig. 5C), accounting for the peak of the fall bloom as measured by bulk chlorophyll (Fig. 11B). Previous studies have indicated that this is also the time of maximum tintinnid abundance (62), microzooplankton biovolume (58), microbial biomass as measured by particulate ATP (58), and biomass of the copepods *Pseudocalanus*, *Acartia*, and *Oithona* (63). Observations of viruses, bacteria, phytoplankton, and zooplankton made in the English Channel from October 1992 to January 1994 show similar summer developments of plankton biomass (7).

From the autumn equinox to the winter solstice, the stratification of the water column begins to be eroded by lower air temperatures and stronger winds, bringing nutrients to the surface (Figs. 3D–F). However, increased river discharge (Fig. 3C) and lower surface salinity (Fig. 3B) retard the destratification. Before the solar radiation becomes too low, there is an opportunity for moderate phytoplankton renewal. This is evident as shoulders centered at week 44 in the plots of abundance (Figs. 5A,D) and chlorophyll (Fig. 11B). In 1974, the bloom at this time of year was the dinoflagellate *Ceratium longipes* (64). After the winter solstice, the water column is destratified completely and the microbial populations, excepting *Synechococcus*, reach their annual minima.

The average 52-week cycle of microbial abundance is summarized as high in the summer and low in the winter. We demonstrated previously how the heterotrophic bacteria and *Synechococcus* in Bedford Basin appear to fit a global pattern in which their annual average abundance is correlated to the annual average temperature (17). On a weekly basis, however, Bedford Basin populations do not track directly water temperature. At this shorter time scale, we surmise that the control of abundance is effected by an interplay among "bottom up" (nutrients), "top down" (grazing), and "side in" (viral lysis) factors. For example, in the Bay of Blanes in the northwest Mediterranean Sea, Agawin et al. (65) showed that the observed seasonal variation in *Synechococcus* abundance is the result of a varying balance between production and loss processes. In summer, there is an excess of unconsumed production whereas in winter, there is none. Studies in Boothbay Harbor (66) and the English Channel (7) also indicate high abundances of *Synechococcus* in late summer, but not in direct parallel with the seasonal development of water temperature. In Bedford Basin, we do not have measurements of the rates of production and loss for any of the microbial groups, but it can be accepted readily that the net result of these processes must give rise to the observed microbial stocks.

For bacteria and viruses, the general patterns of seasonal variation in the Basin are similar to those reported elsewhere (7,9,17) and reflect the trophic dependence of these microbial partners on each other and on the phytoplankton. Interactions among these microbes occur at time scales of hours or days, but the outcome of these events is integrated on the weekly time scale of our monitoring program. In discriminating between subpopulations of bacteria by the intensity of DNA fluorescence (i.e., HDNA versus LDNA), we are unable to discern a clear seasonal trend in bacterial percentage composition over the 52-week cycle (Fig. 10A). The earlier portion of the time series (15) hinted at a lower percentage in summer of the HDNA bacteria, which are presumed to be the larger, more active bacteria (31). The average range of percent HDNA in Bedford Basin (58%–78%) is confined to the high end of the full range (~20%–90%) seen across a diversity of water bodies (15), emphasizing the productive nature of this eutrophic inlet. In mesocosm experiments, Gasol et al. (31) showed that heterotrophic nanoflagellates can shift a bacterial assemblage to a lower percent HDNA composition. This is consistent with the known selective grazing behavior of flagellates on the larger, more active bacteria. In the absence of contemporaneous measurements of bacterial grazers in Bedford Basin, we are unable to assess the presumptive link between grazing activity and bacterial population structure. We note, however, that LDNA bacteria in Bedford Basin are not inactive, as they also show an annual maximum in the summer (Fig. 9C). By one account, they grow more than three times more slowly than HDNA bacteria (15). The specific rate of ^{3}H-leucine incorporation measured in flow-sorted bacteria ranged from 3 to 74-fold greater in HDNA bacteria than in LDNA bacteria (67). Perhaps the rates of LDNA cell loss to grazers and viral destruction are commensurately slower as well.

Viral infection of host bacteria or algae proceeds very quickly and may result in host mortality of up to 50% per

day (8,9). In the course of these short-term events, there can be an inverse relationship between host and parasite abundance. However, at longer time scales, or larger spatial scales, the relationship is positive. A tight coupling between bacteria and virus in Bedford Basin is evidenced by parallel variations at the weekly time scale (Fig. 9). The virus-to-bacteria ratio (VBR) is higher in the spring and summer (Fig. 10C), suggesting a seasonal shift to higher host mortality even as the hosts increase. In discriminating between subpopulations of virus by the intensity of DNA fluorescence (i.e., V-I versus V-II), we are unable to discern a clear seasonal trend in viral percentage composition over the 52-week cycle (Fig. 10B). However, the biological distinction between V-I and V-II is obscure. Marie et al. (33) speculated that V-I might be infectious to phytoplankton, whereas V-II might be infectious to heterotrophic bacteria. This hypothesis has yet to be tested. In fact, the green fluorescence intensity of SYBR-stained viruses is not related linearly to their genome size (34). Notwithstanding these uncertainties in the viral subpopulations, the total VBR in Bedford Basin is similar to values found elsewhere (9), indicating the potential for an active repeated shunt of material from bacteria to viruses to dissolved organic matter and back to bacteria, with a build up of bacterial respiratory losses. The smallness of the virus standing stock (Table 1) belies the significant impact of viruses on the recycling of nutrients and carbon (69).

In summary, the surface waters of Bedford Basin exhibit general features common to many coastal plankton systems dominated by phytoplankton biomass and production. A major bloom of phytoplankton biomass in spring is fueled by nitrate, a lower but sustained level of phytoplankton biomass in summer is fueled by recycling activities of bacteria and viruses, a secondary bloom of phytoplankton biomass develops in autumn, and a return to lowest community biomass occurs in winter (Table 1). A weekly inventory of the microbial community by FCM counts of single cells shows that populations reach their numerical apex between the summer solstice and the autumn equinox. This is the pivotal period for a program designed to monitor the long-term annual changes of the microbial community in Bedford Basin.

ACKNOWLEDGMENTS

We are grateful to all who have helped to sustain the weekly sampling and the analyses of samples. In particular, we thank Jeff Spry, Edward Horne, Jay Bugden, Jeff Anning, Pierre Clement, and Tim Perry. We appreciate the helpful comments provided by Glen Harrison, Trevor Platt, and Kenneth Mann.

LITERATURE CITED

1. Colijn F. The temporal variability of plankton and their physicochemical environment. ICES J Mar Sci 1998;55:557–561.
2. Malone TC, Cole M. Toward a global scale coastal ocean observing system. Oceanography 2000;13:7–11.
3. Therriault JC, Petrie B, Pepin P, Gagnon J, Gregory D, Helbig J, Herman A, Lefaivre D, Mitchell M, Pelchat B, Runge J, Sameoto D. Proposal for a northwest Atlantic zonal monitoring program. Can Tech Rep Hydrogr Ocean Sci 1998;194:1–58.
4. Karentz D, Smayda T. Temperature and seasonal occurrence patterns of 30 dominant phytoplankton species in Narragansett Bay over a 22-year period (1959–1980). Mar Ecol Prog Ser 1984;18:277–293.
5. Radach G, Berg J, Hagmeier E. Long-term changes of the annual cycles of meteorological, hydrographic, nutrient and phytoplankton time series at Helgoland and at LV ELBE 1 in the German Bight. Cont Shelf Res 1990;10:305–328.
6. Mann KH. Ecology of coastal waters: with implications for management, 2nd edition. Oxford: Blackwell Science; 2000.
7. Rodríguez F, Fernández E, Head RN, Harbour DS, Bratbak G, Heldal M, Harris RP. Temporal variability of viruses, bacteria, phytoplankton and zooplankton in the western English Channel off Plymouth. J Mar Biol Ass UK 2000;80:575–586.
8. Fuhrman J. Marine viruses and their biogeochemical and ecological effects. Nature 1999;399:541–548.
9. Wommack KE, Colwell RR. Virioplankton: viruses in aquatic ecosystems. Microbiol Mol Biol Rev 2000;64:69–114.
10. Li WKW. Bedford Basin plankton monitoring program: a weekly record of phytoplankton, bacterioplankton, virioplankton, nutrients, temperature, salinity and oxygen at the deepest point of the Halifax Harbour inlet system. 2000; Internet web site www.mar.dfo-mpo.gc.ca/science/ocean/BedfordBasin/BedfordBasin.htm
11. Harrison WG, Platt T. Variations in assimilation number of coastal marine phytoplankton: effects of environmental co-variates. J Plankton Res 1980;2:249–260.
12. Sinclair M, Subba Rao DV, Couture R. Phytoplankton temporal distributions in estuaries. Oceanol Acta 1981;4:239–246.
13. Smith JC, Platt T, Harrison WG. Photoadaptation of carboxylating enzymes and photosynthesis during a spring bloom. Prog Oceanogr 1983;12:425–459.
14. Lewis MR, Horne EPW, Cullen JJ, Oakey NS, Platt T. Turbulent motions may control phytoplankton photosynthesis in the upper ocean. Nature 1984;311:49–50.
15. Li WKW, Jellett JF, Dickie PM. DNA distributions in planktonic bacteria stained with TOTO or TO-PRO. Limnol Oceanogr 1995;40:1485–1495.
16. Li WKW. Cytometric diversity in marine ultraphytoplankton. Limnol Oceanogr 1997;42:874–880.
17. Li WKW. Annual average abundance of heterotrophic bacteria and *Synechococcus* in surface ocean waters. Limnol Oceanogr 1998;43:1746–1753.
18. Strain PM, Clement PM. Nutrient and dissolved oxygen concentrations in the Letang Inlet, New Brunswick, in the summer of 1994. Can Data Rept Fish Aquat Sci 1996;1004:1–33.
19. Vaulot D, Courties C, Partensky F. A simple method to preserve oceanic phytoplankton for flow cytometric analysis. Cytometry 1989;10:629–635.
20. Li WKW. Experimental approaches to field measurements: methods and interpretation. Can Bull Fish Aquat Sci 1986;214:251–286.
21. Olson RJ, Zettler ER, DuRand MD. Phytoplankton analysis using flow cytometry. In: Kemp PF, Sherr BF, Sherr EB, Cole JJ, editors. Handbook of methods in aquatic microbial ecology. Boca Raton, FL: Lewis; 1993. p 175–186.
22. Marie D, Partensky F, Vaulot D, Brussaard C. Enumeration of phytoplankton, bacteria, and viruses in marine samples. In: Robinson JP, Darzynkiewicz Z, Dean PN, Orfao A, Rabinovitch PS, Stewart CC, Tanke HJ, Wheeless LL, editors. Current protocols in cytometry. Supplement 10, Unit 11.11. New York: John Wiley & Sons; 1999. p 1–15.
23. Chisholm SW. Phytoplankton size. In: Falkowski PG, Woodhead AD, editors. Primary productivity and biogeochemical cycles in the sea. New York: Plenum Press; 1992. p 213–237.
24. Partensky F, Hess WR, Vaulot D. *Prochlorococcus*, a marine photosynthetic prokaryote of global significance. Micro Mol Biol Rev 1999;63:106–127.
25. Collier JL. Flow cytometry and the single cell in phycology. J Phycol 2000;36:628–644.
26. Li WKW. Composition of ultraphytoplankton in the central North Atlantic. Mar Ecol Prog Ser 1995;122:1–8.
27. Verity PG, Robertson CY, Tronzo CR, Andrews MG, Nelson JR, Sieracki ME. Relationships between cell volume and the carbon and nitrogen content of marine photosynthetic nanoplankton. Limnol Oceanogr 1992;37:1434–1446.
28. Li WKW, Dickie PM, Harrison WG, Irwin BD. Biomass and production of bacteria and phytoplankton during the spring bloom in the western North Atlantic Ocean. Deep Sea Res II 1993;40:307–327.
29. Del Giorgio PA, Bird DF, Prairie YT, Planas D. Flow cytometric determination of bacterial abundance in lake plankton with the green nucleic acid stain SYTO 13. Limnol Oceanogr 1996;41:783–789.
30. Marie D, Partensky FP, Jacquet S, Vaulot D. Enumeration and cell cycle analysis of natural populations of marine picoplankton by flow

cytometry using the nucleic acid stain SYBR Green I. Appl Environ Microbiol 1997;63:186–193.
31. Gasol JM, Zweifel UL, Peters F, Fuhrman JA, Hagström Å. Significance of size and nucleic acid content heterogeneity as measured by flow cytometry in natural planktonic bacteria. Appl Environ Microbiol 1999;65:4475–4483.
32. Gasol JM, del Giorgio PA. Using flow cytometry for counting natural planktonic bacteria and understanding the structure of planktonic bacterial communities. Sci Mar 2000;64:197–224.
33. Marie D, Brussaard CPD, Thyrhaug R, Bratbak G, Vaulot D. Enumeration of marine viruses in culture and natural samples by flow cytometry. Appl Environ Microbiol 1999;65:45–52.
34. Brussaard CPD, Marie D, Bratbak G. Flow cytometric detection of viruses. J Virol Methods 2000;85:175–182.
35. Harrison WG, Platt T, Petrie B, Sathyendranath S. Variability in phytoplankton biomass on the Scotian Shelf as viewed from space: imagery from the CZCS ocean color sensor (1978–1986) and SeaWiFS (1997-present). In: Bell CR, Brylinsky M, Johnson-Green P, editors. Microbial biosystems: new frontiers, Eighth International Symposium on Microbial Ecology. Halifax: Atlantic Canada Society for Microbial Ecology; 2000. p 531–539.
36. Reckermann M, Colijn F, editors. Aquatic flow cytometry: achievements and prospects. Sci Mar 2000;64:117–268.
37. Hofstraat JW, van Zeijl WJM, de Vreeze MEJ, Peeters JCH, Peperzak L, Colijn F, Rademaker TWM. Phytoplankton monitoring by flow cytometry. J Plankton Res 1994;16:1197–1224.
38. DuRand MD, Olson RJ, Chisholm SW. Phytoplankton population dynamics at the Bermuda Atlantic Time-Series Station in the Sargasso Sea. Deep Sea Res II 2001;48:1983–2003.
39. Olson RJ, Sosik H. An in situ flow cytometer for the optical analysis of individual particles in seawater. American Society for Limnology and Oceanography, 1999 meeting abstract, Santa Fe.
40. Dubelaar GBJ, Gerritzen PL. Cytobuoy: a step forward towards using flow cytometry in operational oceanography. Sci Mar 2000;64:255–265.
41. Lim EL, Amaral LA, Caron DA, DeLong EF. Application of rRNA-based probes for observing marine nanoplanktonic protists. Appl Environ Microbiol 1993;59:1647–1655.
42. Rice J, Sleigh MA, Burkill PH, Tarran GA, O'Connor CD, Zubkov MV. Flow cytometric analysis of characteristics of hybridization of species-specific fluorescent oligonucleotide probes to rRNA of marine nanoflagellates. Appl Environ Microbiol 1997;63:938–944.
43. Vives-Rego J, Guindulain T, Latatu A, García A, Iriberri J, Comas J. Cytometric detection and quantification of heterotrophic nanoflagellates. In: Measurement of microbial activities in the carbon cycle in aquatic environments. Noordwijkerhout: 7th European Marine Microbiology Symposium. 2000. p 117.
44. Platt T, Prakash A, Irwin B. Phytoplankton nutrients and flushing of inlets on the coast of Nova Scotia. Natural Can 1972;99:253–261.
45. Mitchell MR. The influence of local wind forcing on the low-frequency variations of chlorophyll *a* in a small marine basin. Cont Shelf Res 1991;11:53–66.
46. Lewis MR, Platt T. Scales of variability in estuarine ecosystems. In: Kennedy VS, editor. Estuarine comparisons. New York: Academic Press; 1982. p 3–20.
47. Amadi I, Subba Rao DV, Pan Y. A *Gonyaulax digitale* red water bloom in the Bedford Basin, Nova Scotia, Canada. Bot Mar 1992;35:451–455.
48. Subba Rao DV, Pan Y, Zitko V, Bugden G, Mackeigan K. Diarrhetic shellfish poisoning (DSP) associated with a subsurface bloom of *Dinophysis norvegica* in Bedford Basin, eastern Canada. Mar Ecol Prog Ser 1993;97:117–126.
49. Petrie B, Yeats P, Strain P. Nitrate, silicate and phosphate atlas for the Scotian Shelf and the Gulf of Maine. Can Tech Rep Hydrogr Ocean Sci 1999;203:1–96.
50. Mann KH. Relationship between morphometry and biological functioning in three coastal inlets of Nova Scotia. In: Cronin EL, editor. Estuarine research, Volume 1: chemistry, biology, and the estuarine system. New York: Academic Press; 1975. p 634–644.
51. Taguchi S, Platt T. Phytoplankton biomass in Bedford Basin: volume, surface area, carbon content and size distribution. Fish Mar Serv Data Rep 1978;55:1–404.
52. Lehman PW. Comparison of chlorophyll *a* and carotenoid pigments as predictors of phytoplankton biomass. Mar Biol 1981;65:237–244.
53. Reid PC. Continuous plankton records: changes in the composition and abundance of the phytoplankton of the north-eastern Atlantic Ocean and North Sea, 1958-1974. Mar Biol 1977;40:337–339.
54. Gieskes WWC, Kraay GW. Dominance of cryptophyceae during the phytoplankton spring bloom in the central North Sea detected by HPLC analysis of pigments. Mar Biol 1983;75:179–185.
55. Subba Rao DV, Smith SJ. Temporal variation of size-fractionated primary production in Bedford Basin during the spring bloom. Oceanol Acta 1987;1:101–109.
56. Jeffrey SW, Vesk M. Introduction to marine phytoplankton and their pigment signatures. In: Jeffrey SW, Mantoura RFC, Wright SW, editors. Phytoplankton pigments in oceanography: guidelines to modern methods. Paris: UNESCO Publishing; 1997. p 37–84.
57. Kepkay PE, Niven SEH, Jellett JF. Colloidal organic carbon and phytoplankton speciation during a coastal bloom. J Plankton Res 1997;19:369–389.
58. Taguchi S, Platt T. Size distribution and chemical composition of particulate matter in Bedford Basin, 1973 and 1974. Fish Mar Serv Data Rep 1978;56:1–370.
59. Harrison WG. Uptake and recycling of soluble reactive phosphorus by marine microplankton. Mar Ecol Prog Ser 1983;10:127–135.
60. Platt T. Analysis of the importance of spatial and temporal heterogeneity in the estimation of annual production by phytoplankton in a small enriched marine basin. J Exp Mar Biol Ecol 1975;18:99–109.
61. Irwin B. Coulometric measurement of primary production, with comparison against dissolved oxygen and ^{14}C methods in a seasonal study. Mar Ecol Prog Ser 1991;71:97–102.
62. Paranjape MA. The seasonal cycles and vertical distribution of tintinnines in Bedford Basin, Nova Scotia, Canada. Can J Zool 1987;65:41–48.
63. Sameoto DD. Macrozooplankton biomass measurements in Bedford Basin, 1969-1971. Fish Res Bd Can Tech Rep 1971;282:1–238.
64. Taguchi S. Seasonal studies of the dinoflagellate *Ceratium longipes* (Bailey) Gran in the Bedford Basin, Canada. J Exp Mar Biol Ecol 1981;55:115–131.
65. Agawin NSR, Duarte CM, Agustí S. Growth and abundance of *Synechococcus* sp. in a Mediterranean bay: seasonality and relationship with temperature. Mar Ecol Prog Ser 1998;170:45–53.
66. Shapiro LP, Haugen EM. Seasonal distribution and temperature tolerance of *Synechococcus* in Boothbay Harbor, Maine. Est Coast Shelf Sci 1988;26:517–525.
67. Lebaron P, Servais P, Agogué H, Courties C, Joux F. Does the high nucleic acid content of individual bacterial cells allow us to discriminate between active cells and inactive cells in aquatic systems? Appl Environ Microbiol 2001;67:1775–1782.
68. Fukuda R, Ogawa H, Nagata T, Koike I. Direct determination of carbon and nitrogen contents of natural bacterial assemblages in marine environments. Appl Environ Microbiol 1998;64:3352–3358.
69. Wilhelm SW, Suttle CA. Viruses and nutrient cycles in the sea. Bioscience 1999;49:781–788.